# H(3)(+) emission in the ejecta of SN 1987A

THE ASTROPHYSICAL JOURNAL, 500:1049–1054, 1998 June 20


# $H_3^+$ EMISSION IN THE EJECTA OF SN 1987A

MIN YAN[1,2] AND A. DALGARNO[3]
Harvard-Smithsonian Center for Astrophysics, 60 Garden Street, Cambridge, MA 02138
*Received 1997 October 14; accepted 1998 January 30*

## ABSTRACT

We present a chemical and thermal model of the envelope of SN 1987A. We assume that half of the hydrogen envelope is broken into many dense clumps and mixed into the inner region. For a range of densities and energy deposition rates, we find two phases, one with a temperature of about 7000 K and another with a temperature of about 3000 K. We suggest that the $H_3^+$ features originate in the low-temperature clumps. In them, the cooling is mainly through CO vibrational emission, and the $H_3^+$ vibrational levels are in LTE. Emission features observed at 3.41 and 3.53 $\mu$m can be reproduced satisfactorily by $H_3^+$ fundamental band emission at a temperature of 2000 K when absorption by telluric water vapor is taken into account. The model is successful in predicting the dependence on time of the emission features.

*Subject headings:* atomic processes — infrared: stars — supernovae: individual (SN 1987A)

## 1. INTRODUCTION

The spectra of SN 1987A have provided a wealth of information about the physical conditions in the expanding ejecta (McCray 1993). There remain several unidentified features (Meikle et al. 1993). Two features at 3.409 and 3.533 $\mu$m have been tentatively attributed to vibrationally excited $H_3^+$ (Miller et al. 1992). The chemistry of $H_3^+$ has been explored by Miller et al. (1992), Dalgarno (1993), and Culhane & McCray (1995). Miller et al. (1992) put forward a simple model that indicated that sufficient $H_3^+$ could be formed in the envelope, but in a more comprehensive study, Culhane & McCray (1995) argued the contrary view, finding that the predicted abundance of $H_3^+$ failed by several orders of magnitude to meet that required to explain the strength of the spectral features.

A major reason for the low abundance of $H_3^+$ in the model of Culhane & McCray (1995) is the high temperature of 7000 K at day 200 that they adopted. They inferred the temperature from the intensities of the Ca II doublet lines, which Li & McCray (1993) had shown are produced in the hydrogen-rich gas of the envelope with calcium in the primordial fractional abundance present. At temperatures of 7000 K, $H_2$, from which $H_3^+$ is formed, is thermally dissociated with high efficiency, as is $H_3^+$.

That the identification of $H_3^+$ must fail if the temperature is high is demonstrated also by the predicted emission profile of $H_3^+$. If due to $H_3^+$, the presence of the features at 3.41 and 3.53 $\mu$m and the absence of others to which hot $H_3^+$ would rise place an upper limit of 3000 K on the temperature (Miller et al. 1992).

We suggest that there are temperature inhomogeneities in the envelope and that $H_2$ and $H_3^+$ can be produced in a cooler region and survive in sufficient abundances to explain the emissions.

## 2. IONIZATION, THERMAL, AND CHEMICAL PROCESSES

The mass in the hydrogen-rich envelope of SN 1987A is about 12 $M_\odot$ (Woosley, Pinto, & Weaver 1988). About 6 $M_\odot$ of the gas is mixed into the inner region and broken into high-density clumps (McCray 1993; Li & McCray 1993). The ionization, thermal, and chemical processes are driven by $\gamma$-rays from the decay of radioactive $^{56}$Co.

For the hydrogen chemistry, we adopted the set of reactions listed by Culhane & McCray (1995), supplemented by the destruction of $H_2$ by electron impact dissociation:

$$e + H_2 \rightarrow e + H + H\,. \tag{1}$$

For the $H_3^+$ production from the excited hydrogen atoms H*,

$$H^* + H_2 \rightarrow H_3^+ + e\,, \tag{2}$$

which is the dominant $H_3^+$ formation process when the temperature is under 3000 K, we adopt a rate coefficient of $3 \times 10^{-9}$ cm$^3$ s$^{-1}$ to include the contribution due to H ($2p$) (Chupka, Russell, & Refaey 1968; Glass-Maujean 1989; Terazawa et al. 1993). We took account of the presence of helium, which affects the hydrogen chemistry through the reactions

$$He^+ + H \rightarrow HeH^+ + \nu\,, \tag{3}$$

$$H^+ + He \rightarrow HeH^+ + \nu\,, \tag{4}$$

$$HeH^+ + H \rightarrow H_2^+ + He\,, \tag{5}$$

$$HeH^+ + H_2 \rightarrow H_3^+ + He\,, \tag{6}$$

$$HeH^+ + e \rightarrow He + H\,, \tag{7}$$

$$He^+ + H_2 \rightarrow He + H^+ + H\,. \tag{8}$$

Mixed in the hydrogen-rich clumps are the original heavy elements of the interstellar clouds of the Large Magellanic Cloud. We adopted abundances equal to one-third of the solar values (Arnett et al. 1989). We employed a limited heavy-element chemistry that leads to the formation of CO, OH, $H_2O$, and CH. In addition to ion-molecule reaction sequences initiated by charge transfer from $H^+$ and proton transfer from $H_3^+$ and terminated by dissociative recombination,

$$O + H^+ \rightarrow O^+ + H\,, \tag{9}$$

$$O^+ + H_2 \rightarrow OH^+ + H\,, \tag{10}$$

$$O + H_3^+ \rightarrow OH^+ + H_2\,, \tag{11}$$

[1] yan@cfa160.harvard.edu.
[2] Now at Ritter Observatory, University of Toledo, Toledo, OH 43606.
[3] adalgarno@cfa.harvard.edu.

$$OH^+ + H_2 \rightarrow H_2O^+ + H\,, \quad (12)$$

$$OH^+ + e \rightarrow O + H\,, \quad (13)$$

$$H_2O^+ + e \rightarrow OH + H\,, \quad (14)$$

and similar reactions involving carbon, we included neutral particle reactions such as

$$O + H_2 \rightarrow OH + H\,, \quad (15)$$

$$C + OH \rightarrow CO + H\,. \quad (16)$$

The molecules are destroyed largely through reactions with $H^+$ and $He^+$:

$$OH + H^+ \rightarrow OH^+ + H\,, \quad (17)$$

$$CO + He^+ \rightarrow C^+ + O + He\,. \quad (18)$$

We ignored the destructive effects of external ultraviolet radiation, assuming that $H_2$ and CO are self-shielding and that the radiation is absorbed mostly by metals. The effects of internally generated metastable H and He two-photon emission will be discussed later in this section. The set of reactions and their rate coefficients may be obtained from the compilation of Millar, Farquhar, & Willacy (1997).

The relative roles of ion-molecule and neutral particle chemistry depend on the temperature, which was calculated from a balance between heating and cooling. The heat deposited in the hydrogen-rich envelope by $\gamma$-rays was calculated from the data of Yan, Liu, & Dalgarno (1998), who computed the heat arising from energetic electrons traversing an ionized gas mixture of $H_2$, H, and He. In the ejecta, quenching of hydrogen atoms in the $n = 2$ states is an additional source of heat. There are two possible phases, a hot atomic phase and a cooler warm molecular phase. In the molecular phase, exothermic chemical reactions deposit heat into the gas (Glassgold & Langer 1973).

The cooling radiation in the hot gas is emitted in lines of $Ca^+$ and $Fe^+$. Electron impact excitation rate coefficients are given for $Ca^+$ by Li & McCray (1993) and for $Fe^+$ by Pradhan & Berrington (1993), Pradhan & Zhang (1993), and Zhang & Pradhan (1995). The cooling of the warm molecular gas is primarily due to excitation of the vibrational levels of CO, $H_3^+$, and $H_2$ and the rotational levels of OH and CO. We obtained the rate coefficients for excitation of the rotational levels by electron impact of CO and OH following Dickinson et al. (1977). For rotational excitation of CO by hydrogen atom collisions, we constructed rate coefficients from the calculations of Chu & Dalgarno (1975) and Green, Pan, & Bowman (1995), and for rotational excitation of OH, we used the results of Field (1982). For vibrational excitation of $H_2$ by electron impact, we used the results of England, Elford, & Crompton (1988), Buckman et al. (1990), and Rescigno, Elza, & Lengsfield (1993); for vibrational excitation of CO, we followed the prescription of Liu & Dalgarno (1994). Vibrational excitation of $H_3^+$ occurs mainly by collisions with H atoms. To calculate its contribution to the cooling, we adopted a two-level system and used the rate coefficients of Kim, Fox, & Porter (1992). Vibrational excitation of CO by H atom impact is the major cooling process in the molecular phase. Several experimental and theoretical studies of collisions of H with CO have been carried out (Ayres & Wiedemann 1989; Green, Pan, & Bowman 1995). We followed the formulation of Neufeld & Kaufman (1993) with rate coefficients constructed to be consistent with the shock tube data of Glass & Kironde (1982), the hot atom study of Geiger, Schatz, & Harding (1985), and the calculations of Green, Pan, & Bowman (1995). Considerable uncertainties remain in the rate coefficients, but their influence on the derived temperatures is small. Because photon trapping in the optically thick medium significantly lengthens the effective radiative lifetimes, collisions are fast enough to bring the level populations into local thermodynamic equilibrium. We took account of photon trapping using the Solobev formalism as described by Xu et al. (1992). The cooling efficiency is then determined by the radiative properties of CO, which are listed in Goorvitch & Chakerian (1994a, 1994b) and Huré & Roueff (1996).

At day 192, the average density in a gas clump is $2 \times 10^{11}$ $cm^{-3}$, and the average energy deposition rate is $1 \times 10^{-5}$ eV $s^{-1}$ per H atom (Xu et al. 1992; Kozma & Fransson 1992; Li & McCray 1993). Fluctuations may occur. We present in Figure 1 the calculated abundances of $H_3^+$ for an energy deposition rate of $1 \times 10^{-5}$ eV $s^{-1}$ per hydrogen atom for a range of densities. We find that for densities between $6 \times 10^{11}$ and $4 \times 10^{10}$ $cm^{-3}$, there are two solutions. In one phase, the gas is hot with a temperature of 7000 K, an electron density of $4 \times 10^8$ $cm^{-3}$, and a negligible abundance of $H_3^+$, as in the model of Culhane & McCray (1995), and in the other phase, the gas is warm with a temperature of 3000 K, an electron density of $1 \times 10^8$ $cm^{-3}$, and a fractional abundance of $H_3^+$ of $6 \times 10^{-8}$. We refer to these two phases as phase A and phase B respectively. Lepp & McCray (1983) had earlier discovered the existence of two phases in cosmic gas irradiated by X-rays. Phase B disappears at densities below $4 \times 10^{10}$ $cm^{-3}$ or above $6 \times 10^{11}$ $cm^{-3}$. In phase B, the heat input is $4.8 \times 10^{-6}$ eV $s^{-1}$ per H atom, divided nearly equally between fast electron Coulomb heating and dissociative recombination of $OH^+$ and $H_2O^+$, with the remainder from electron quenching of excited hydrogen atoms and the reaction of H(2) with $H_2$ producing $H_3^+$ followed by dissociative recombination.

Photodissociation may occur by absorption of photons emitted in the two-photon decay of metastable hydrogen and helium. In phase B, destruction of $H_2$ by photodissociation is slow compared to destruction by reactions with excited hydrogen atoms and with $H^+$, and photodissociation of CO and other molecules is limited by the strong shielding due to H, $H_2$, and metals. In phase A, photodissociation is more significant (Culhane & McCray 1995), but even in its absence, molecules are unimportant constituents of the gas.

In Figure 2, we present the calculated abundances of $H_3^+$ for the average density of $2 \times 10^{11}$ $cm^{-3}$ as a function of the energy deposition rate. For energy deposition rates between $4.1 \times 10^{-7}$ and $1.1 \times 10^{-5}$ eV $s^{-1}$ per H atom, two equilibrium phases are again possible. For energy deposition rates below $4.1 \times 10^{-7}$ eV $s^{-1}$ per H atom, only phase B exists, and above $1.1 \times 10^{-5}$ eV $s^{-1}$ per H atom, only phase A exists.

Whether a gas clump is in phase A or phase B depends on its history. At early times, because of the large $\gamma$-ray optical depth of the ejecta, the energy deposition rate in regions outside the iron core increases with time. Thus a clump initially in phase A will remain in phase A, whereas a clump initially in phase B may remain in phase B, or it may jump to phase A at later times when the energy deposition rate is high enough.

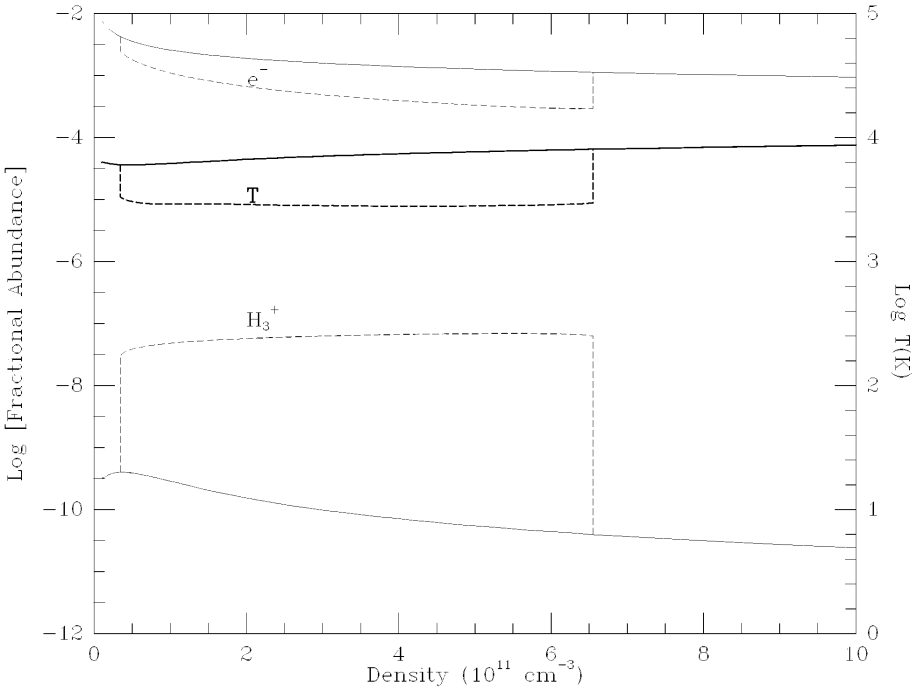


FIG. 1.—Steady state fractional abundances of $H_3^+$ and electrons and the temperature at day 192 for hydrogen clumps as functions of density. The energy deposition rate is assumed to be the global average value, $1 \times 10^{-5}$ eV s$^{-1}$ per H atom. The solid lines are phase A, and the dashed lines are phase B.

To investigate the evolution of phase B gas clumps, we adopted at day 192 an average density of $3 \times 10^{11}$ cm$^{-3}$ varying with time as $t^{-3}$, an average energy deposition rate of $0.3 \times 10^{-5}$ eV s$^{-1}$ varying after day 192 as exp $(-t/111.3)$ with $t$ measured in days, and a total mass of 1.2 $M_\odot$, which is the amount of warm hydrogen needed to produce the appropriate amount of $H_3^+$. Before day 192, we assumed the energy deposition rate was reduced by a factor exp $[-0.6(\tau - \tau_0)]$, where $\tau$ is the $\gamma$-ray opacity, and $\tau_0$ is its value at day 192. The $\gamma$-ray photons can escape directly after day 300 (Xu et al. 1992), so that $\tau_0$ is approximately unity.

In Figure 3, we present the calculated fractional abundances of $H_2$, H ($n = 2$), $H_3^+$, CO, and OH, together with the electron fraction and the temperature from day 100 to day 500. During this period, the clumps are mostly atomic

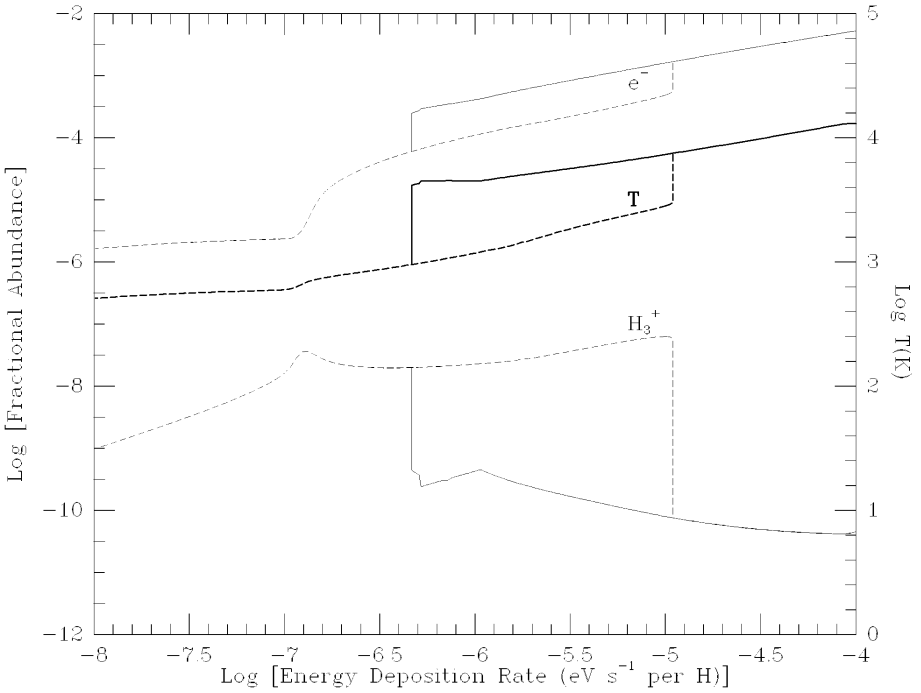


FIG. 2.—Fractional abundances of $H_3^+$ and electrons and the temperature at day 192 for hydrogen clumps as functions of the energy eposition rate. The density is assumed to be the global average value, $n_H = 2 \times 10^{11}$ cm$^{-3}$. The solid lines are phase A, and the dashed lines are phase B.

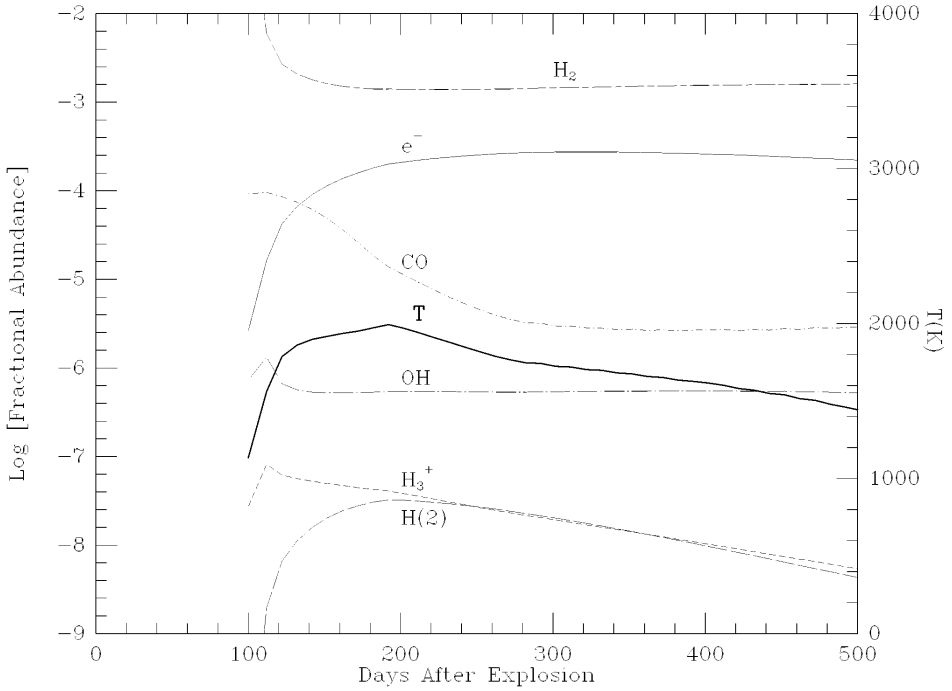


FIG. 3.—Fractional abundances of $H_2$, H(2), $H_3^+$, CO, OH, and electrons and the temperature of phase B hydrogen clumps as functions of time

hydrogen. The $H_2$ fractional abundance decreases from $1 \times 10^{-2}$ to $2 \times 10^{-3}$, the temperature increases from 1400 K to a maximum of 2000 K and then decreases slowly to 1400 K, and the fractional abundance of $H_3^+$ decreases from $1 \times 10^{-7}$ to $5 \times 10^{-9}$. The total mass in $H_3^+$ at day 192 is $1.6 \times 10^{-7}\ M_\odot$.

The predicted abundances of CO and OH are shown in Figure 3. Carbon monoxide decreases from a fractional abundance of $1 \times 10^{-4}$ to $3 \times 10^{-6}$, and OH remains close to an abundance of $5 \times 10^{-7}$. The total mass of CO at day 192 is $4 \times 10^{-4}\ M_\odot$, which is an order of magnitude less than the amount thought to exist in the region where C and O are abundant (Liu & Dalgarno 1995). Despite the lower mass of CO in the warm hydrogen clumps, the CO emission from them is a significant fraction, as much as one-half, of the total CO emission from the ejecta, which is about 2% of the bolometric luminosity (Meikle et al. 1989; Bouchet & Danziger 1993; Wooden et al. 1993).

The $H_2$ (1–0) $S(1)$ emission intensity in our model at day 377 is 3 orders of magnitude smaller than the observational upper limit (Culhane & McCray 1995), which is consistent with the nondetection of other $H_2$ infrared lines. Thus the broad weak feature in the 2.11–2.15 $\mu$m range observed by Meikle et al. (1993) before day 500 may be due entirely to [Fe II] 2.133 $\mu$m emission.

Figure 3 shows that H clumps may have temperatures of about 1000 K. Grains may be formed. The presence of grains would enhance the $H_2$ and $H_3^+$ abundances.

## 3. $H_3^+$ EMISSION SPECTRUM

The radiative lifetimes of the levels of $H_3^+$ that give rise to features at 3.41 and 3.53 $\mu$m are about $6 \times 10^{-3}$ s (Kao et al. 1991). The rate coefficient for quenching of the levels by hydrogen atoms is about $3 \times 10^{-9}$ cm$^3$ s$^{-1}$ (Kim, Fox, & Porter 1992) so that at a density of $3 \times 10^{11}$ cm$^{-3}$, the levels will be close to local thermodynamic equilibrium. Figure 4 shows the $H_3^+$ spectrum corresponding to a temperature of 2000 K and an expansion velocity of 2350 km s$^{-1}$ superposed on the background continuum from Miller et al. (1992) together with the spectrum observed by Meikle et al. (1989). The mass of $H_3^+$ required to match the measured intensity is $1.6 \times 10^{-7}\ M_\odot$.

The mass of $H_3^+$ and the temperature are close to the theoretical values we obtained for phase B gas clumps, but there is an apparent serious mismatch of the spectrum. The features at 3.53 and 3.41 $\mu$m are reproduced satisfactorily, the small discrepancy for the 3.41 $\mu$m features being attributable to a contribution from the $5\ ^2S$–$4\ ^2P$ doublet of sodium suggested by Lucy et al. (1991), but the predicted strong emissions at 3.02, 3.20, and 3.26 $\mu$m are not present in the observed spectra. They would be much weaker if the temperature were 1500 K or less, but their absence may be a consequence of strong telluric water vapor absorption in the $0$–$2\nu_2$, $0$–$\nu_1$, and $0$–$\nu_3$ bands (Meikle et al. 1989; Rothman et al. 1992), which occur in the same spectral regions. Figure 5 shows the same theoretical spectrum but with the inclusion of absorption by 3 cm precipitable telluric water vapor broadened by collisions at a collision frequency of $1.5 \times 10^9$ s$^{-1}$. The three features at 3.02, 3.20, and 3.26 $\mu$m disappear.

The spectral shape of the 3.53 $\mu$m emission feature appears to change from sharp-peaked at day 110 to flat-topped at day 345 (Meikle et al. 1989), in contrast to the profiles of the atomic hydrogen recombination lines (Hanuschik et al. 1993; Spyromilio, Stathakis, & Meurer 1993). The behavior may be a consequence of the increase in the local energy deposition rate as the ejecta expands, causing a transition of some of phase B hydrogen clumps into phase A hydrogen clumps.

Table 1 lists the measured and predicted strengths of the 3.53 $\mu$m feature from day 110 to day 349, expressed as ratios to the strength of the feature at day 192. The agreement is

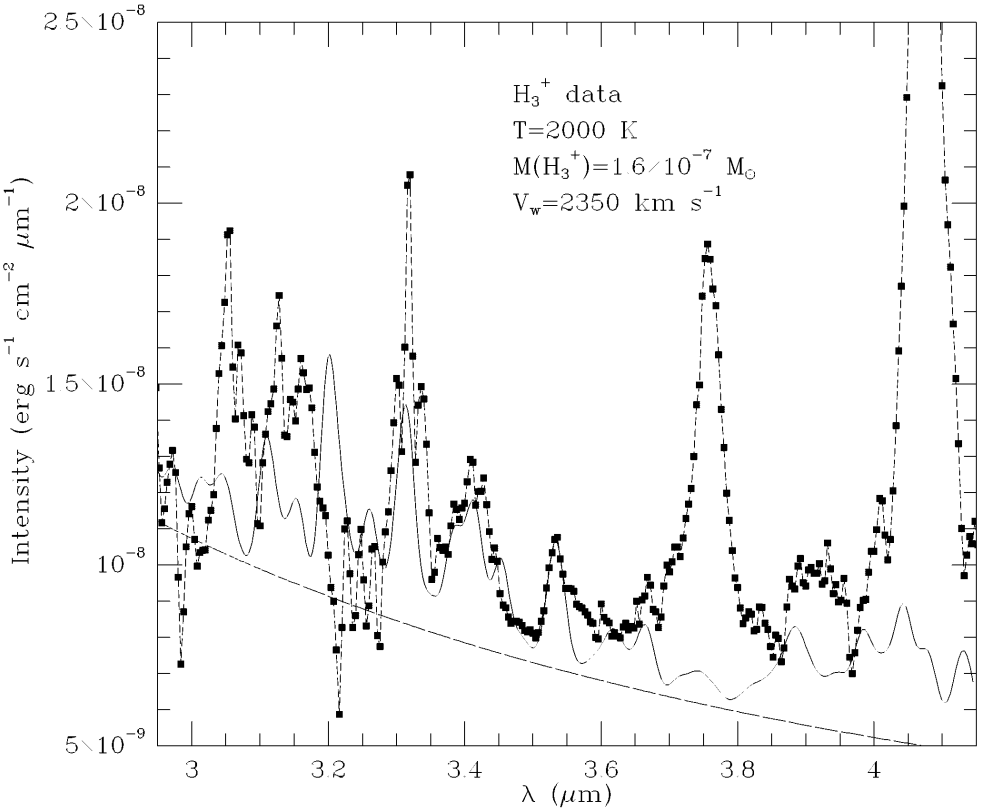


FIG. 4.—Fit of the computed $H_3^+$ $v_2 \rightarrow 0$ spectrum (*solid curve*) to the spectrum of SN 1987A on day 192 (Meikle et al. 1989) (*filled squares*) from 2.95 to 4.15 $\mu$m. $T$, $V_w$ and $M(H_3^+)$ are the temperature, velocity width at half-maximum, and total $H_3^+$ mass for phase B hydrogen clumps, respectively. The long dashed line is the background continuum. Atmospheric water vapor absorption is not considered.

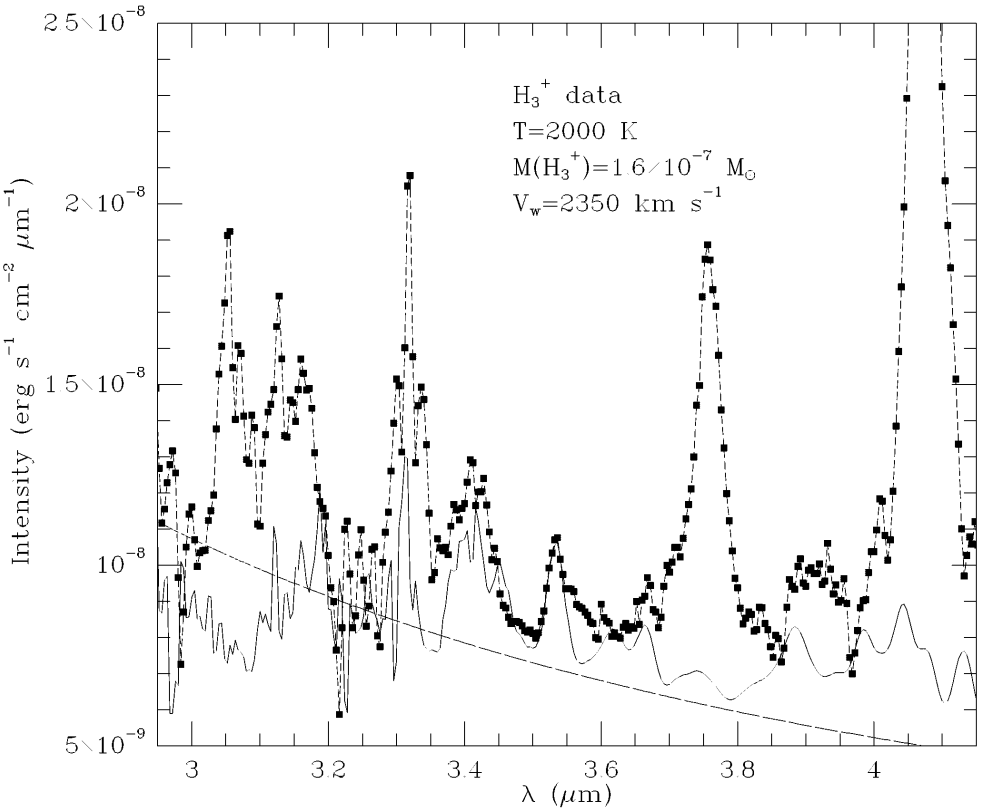


FIG. 5.—Same as for Fig. 4, except that the absorption by atmospheric water vapor is taken into account

TABLE 1

RELATIVE INTENSITY OF THE 3.53 $\mu$m PEAK SCALED TO 1.0 AT DAY 192

| Epoch (days) | Observation | Theory |
|---|---|---|
| 110..... | 1.4 | 1.4 |
| 192..... | 1.0 | 1.0 |
| 255..... | 0.4 | 0.46 |
| 284..... | 0.3 | 0.31 |
| 349..... | 0.1 | 0.14 |

close, and the comparison provides additional support for the identification of $H_3^+$ as the source of the 3.41 and 3.53 $\mu$m emission features in the ejecta of SN 1987A.

We thank Kelly Chance for helpful discussions of the telluric water vapor absorption. We acknowledge support from the National Science Foundation, Division of Astronomical Sciences.

REFERENCES

Arnett, W. D., Bahcall, J. N., Kirshner, R. P., & Woosley, S. 1989, ARA&A, 27, 629
Ayres, T. R., & Wiedeman, G. R. 1989, ApJ, 338, 1033
Bouchet, P., & Danziger, I. J. 1993, A&A, 273, 451
Buckman, S. J., et al. 1990, Phys. Rev. Lett., 65, 3253
Chu, S., & Dalgarno, A. 1975, Proc. R. Soc. London A, 342, 191
Chupka, W. A., Russell, M. E., & Refaey, K. 1968, J. Chem. Phys., 48, 1518
Culhane, M., & McCray, R. 1995, ApJ, 455, 335
Dalgarno, A. 1993, in Dissociative Recombination, ed. B. R. Rowe, J. B. A. Mitchell, & A. Canosa (New York: Plenum), 243
Dickinson, A. S., et al. 1977, A&A, 54, 645
England, J. P., Elford, M. T., & Crompton, R. W. 1988, Australian J. Phys., 41, 573
Field, D. 1982, MNRAS, 201, 527
Geiger, L. C., Schatz, G. C., & Harding, L. B. 1985, Chem. Phys. Lett., 114, 520
Glass, G. P., & Kironde, S. 1982, J. Phys. Chem., 86, 908
Glassgold, A. E., & Langer, W. D. 1973, ApJ, 186, 859
Glass-Maujean, M. 1989, Phys. Rev. Lett., 62, 144
Goorvitch, D., & Chakerian, C. 1994a, ApJS, 91, 483
———. 1994b, ApJS, 92, 311
Green, S., Pan, B., & Bowman, J. M. 1995, J. Chem. Phys., 102, 8800
Hanuschik, R. W., et al. 1993, MNRAS, 261, 909
Huré, J. M., & Roueff, E. 1996, A&AS, 117, 561
Kao, L., Oka, T., Miller, S., & Tennyson, J. 1991, ApJS, 77, 317
Kim, Y. H., Fox, J. L., & Porter, H. S. 1992, J. Geophys. Res., 97, 6093
Kozma, C., & Fransson, C. 1992, ApJ, 390, 602
Lepp, S., & McCray, R. 1983, ApJ, 269, 560
Li, H., & McCray, R. 1993, ApJ, 405, 730
Liu, W., & Dalgarno, A. 1994, ApJ, 428, 769
———. 1995, ApJ, 454, 472
Lucy, L. B., Danziger, I. J., & Gouiffes, C. 1991, A&A, 243, 223
McCray, R. 1993, ARA&A, 31, 175
Meikle, W. P. S., Allen, D. A., Spyromilio, J., & Varani, G. F. 1989, MNRAS, 238, 193
Meikle, W. P. S., et al. 1993, MNRAS, 261, 535
Millar, T. J., Farquhar, P. R. A., & Willacy, K. 1997, A&AS, 121, 139
Miller, S., Tennyson, J., Lepp, S., & Dalgarno, A. 1992, Nature, 355, 420
Neufeld, D. A., & Kaufman, M. J. 1993, ApJ, 418, 263
Pradhan, A. K., & Berrington, K. 1993, J. Phys. B, 26, 157
Pradhan, A. K., & Zhang, H. L. 1993, ApJ, 409, L77
Rescigno, T. N., Elza, B. K., & Lengsfield, B. H. 1993, J. Phys. B, 26, L567
Rothman, L. S., et al. 1992, J. Quan. Spec. Rad. Tran., 48, 469
Spyromilio, J., Stathakis, R. A., & Meurer, G. R. 1993, MNRAS, 263, 530
Terazawa, N., et al. 1993, J. Chem. Phys., 99, 1637
Wooden, D. H., et al. 1993, ApJS, 88, 477
Woosley, S. E., Pinto, P., & Weaver, T. A. 1988, Proc. Astron. Soc. Australia, 7, 355
Xu, Y., McCray, R., Oliva, E., & Randich, S. 1992, ApJ, 386, 181
Yan, M., Liu, W., & Dalgarno, A. 1998, in preparation
Zhang, H. L., & Pradhan, A. K. 1995, A&A, 293, 953